buildings

MDPI

Article

Field Test and Numerical Study of Three Types of Frame Beams Subjected to a 600 kN Anchoring Force

Mengchun Qin [1,†], Guosong Dou [2,†], Jianmin Yang [3,4,*] and Shaowei Wei [5,6]

[1] State Key Laboratory of Hydraulic Engineering Intelligent Construction and Operation, Tianjin University, Tianjin 300350, China; qmc@tju.edu.cn
[2] Beijing Institute of Technology, Beijing 100080, China; 6120220120@bit.edu.cn
[3] School of Civil Engineering, Tianjin University, Tianjin 300350, China
[4] Key Laboratory of Coast Civil Structure Safety of China Ministry of Education, Tianjin University, Tianjin 300350, China
[5] China Academy of Railway Sciences Corporation Limited, Beijing 100080, China; tiandaochouqin97@gmail.com
[6] Beijing Tieke Special Engineering Technological Development Corporation Limited, Beijing 100080, China
* Correspondence: yangjianmin@tju.edu.cn; Tel.: +86-18722172688
† These authors contributed equally to this work.

Abstract: Frame beams with anchor cables constitute a crucial method for slope reinforcement projects. With the development of fabricated structures, there has been an increasing focus on precast prestressed frame beams with anchor cables. This paper presents a field test conducted in Yunnan, China and numerical simulations to analyze the structure behavior of three types of frame beams with a 600 kN anchoring force: cast-in-situ frame beams, precast prestressed frame beams, and precast prestressed frame beams with connections. The results showed that: (1) Although all three types of frame beams met the design requirements for a 600 kN anchoring force capacity, the volume of precast prestressed frame beams constituted only 57% of that of the cast-in-situ frame beams. (2) The maximum bending moment for the precast prestressed frame beams with connections was 60 kN·m less than that for the cast-in-situ frame beams. (3) The field test results for bending moments exceeded the values obtained from the numerical simulation. When using a numerical simulation to study the bending moments of the anchor frame beams, it is acceptable to apply appropriate amplifications to the numerical results. (4) Among the three types of frame beams with cables, the precast prestressed frame beams with connections exhibited the best structural performance.

Keywords: frame beams with anchor cables; cast-in-situ frame beams; precast prestressed frame beams; precast prestressed frame beams with connection; field test; numerical simulation

check for updates

Citation: Qin, M.; Dou, G.; Yang, J.; Wei, S. Field Test and Numerical Study of Three Types of Frame Beams Subjected to a 600 kN Anchoring Force. *Buildings* **2024**, *14*, 401. https://doi.org/10.3390/buildings14020401

Academic Editor: Hassan Karampour

Received: 17 December 2023
Revised: 27 January 2024
Accepted: 30 January 2024
Published: 1 February 2024

Copyright: © 2024 by the authors. Licensee MDPI, Basel, Switzerland. This article is an open access article distributed under the terms and conditions of the Creative Commons Attribution (CC BY) license (https://creativecommons.org/licenses/by/4.0/).

1. Introduction

The anchor frame beam, consisting of frame beams and anchor cables, has been widely used in slope engineering as a new support form [1–4]. The principle of slope reinforcement using frame beams with anchor cables is to maximize the strength of the anchor cables through tensioning and connect the weak structural plane of the rock mass with the stable rock stratum and the frame beam. This reinforcement method aims to improve the overall stability of the slope.

There have been many studies about anchor frame beams with the anchor cable as the research object [5–8]. For example, Li et al. [9] advanced a methodology for determining the layout and length of anchor cables based on three-dimensional geological characteristics. Zhang et al. [10] examined the influence of anchoring orientation and position on reinforcement effectiveness using the global method. Because the loss of anchor cable force is a common occurrence that directly impacts the effectiveness of reinforcement, Shi et al. [11] introduced a novel coupled calculation model to accurately predict the behavior and degree of anchor cable force loss.

As the primary component of anchor frame beams, the frame beams have been the subject of numerous studies [12–15]. For instance, Yuan and Liu [16] established a dynamic simplified model for frame beams with anchor cables to study dynamic response characteristics and the seismic mechanism of the frame beams. Fan et al. [17] devised a new load distribution method intended for calculating internal forces for frame beams. Lian et al. [18] examined the erosion protection provided by frame beams and their impact on stabilization and load-bearing behavior, conducting an analysis of the critical stability conditions of soil particles in a shallow slope under rainfall infiltration. Many studies have also been conducted on the stability of slopes reinforced by anchor frame beams [19–22].

Although the above studies have contributed to the development of anchor frame beams a lot, it should be noted that the majority of frame beams used were cast-in-situ frame beams. With the development of fabricated structures, there has been an increasing focus on precast frame beams. In construction, precast frame beams give the benefits of simplicity, structural stability, and cost-effectiveness when compared with cast-in-situ frame beams [23]. Based on precast frame beams, the Japan Precast Concrete Frame Association [24,25] proposed a novel type of frame beam called precast prestressed frame beams. These beams utilize either the pre-tensioning or post-tensioning technique to introduce prestresses into the precast frame beams. Precast prestressed frame beams with anchor cables present multiple benefits in reinforcement engineering [26,27], but only limited research has been conducted on these novel frame beams with anchor cables.

In this paper, based on the reinforcement project in the Mengping highway in Yunnan, China, a field test and numerical simulations were conducted to investigate the structural performance of three types of frame beams (cast-in-situ frame beams, precast prestressed frame beams, and precast prestressed frame beams with connections; Figure 1) with a 600 kN anchoring force during loading and the normal service period. Precast prestressed frame beams with connections represent an innovative integrated structure created by interconnecting individual precast prestressed frame beams. The results indicated the following: (1) Although three types of frame beams with anchor cables met the design requirements, precast prestressed frame beams had a volume that was only 57% of that of the cast-in-situ frame beams. (2) Precast prestressed frame beams with connections subjected to a 600 kN anchoring force exhibited a maximum bending moment that was 60 kN·m lower than that of the cast-in-situ frame beams. (3) Field test results of bending moments tended to be higher than the numerical results. This indicates the need to appropriately amplify the numerical results when studying the bending moments of anchor frame beams with a numerical simulation. (4) Precast prestressed frame beams with connections demonstrated superior structural performance because they acted as a unified entity, allowing for the transfer of internal forces.

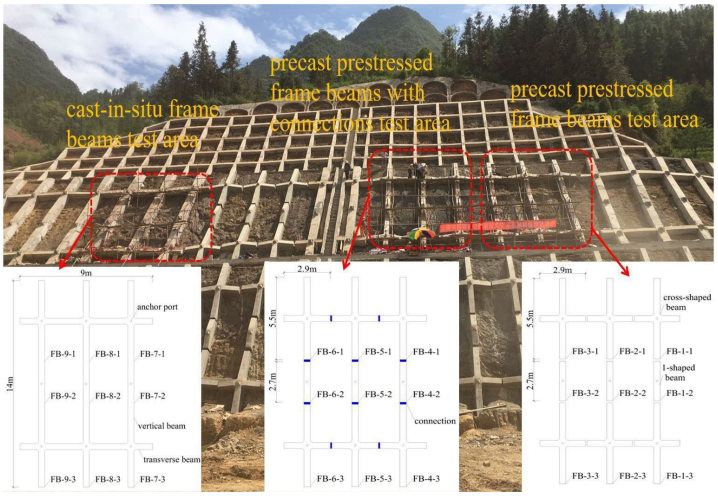


Figure 1. Figure of the field test and schematic diagram of the frame beam layout.

2. Field Test

2.1. Project View

The experimental project took place on a segment of the Mengping highway from 25 + 580 to 25 + 690, located in Yunnan Province, China. The slope comprises four grades, each with a height of 10 m, and the slope ratios ranged from 1:0.75 to 1:1, as illustrated in Figure 1. For this study, a second-grade slope with a 1:1 ratio was selected as the experimental area; the total length of the experimental section was 110 m. The surface of the slope was silty clay, under which lied heavily weathered fractured rock. The soil parameters were obtained by analogy with engineering projects situated in proximate geological conditions (Table 1). The comprehensive friction angle for this structural surface was 33°, while the cohesive strength of the soil–rock interface was determined as 90 kPa. Furthermore, the elastic modulus was specified at 30 MPa.

Table 1. Material parameters in the field test and numerical simulations.

Parameter	Type	Strength (MPa)	Density (kg/m^3)	Young's Modulus (Pa)	Poisson's Ratio	Dilatation Coefficient (1/°C)
Steel reinforcement	Φ	400	7800	2×10^{11}	0.25	—
Prestressed steel strand	φ15.24	1860	7800	2×10^{11}	0.25	1.2×10^{-5}
Concrete	C40	40	2643	3×10^{10}	0.2	—
Soil	—	—	2000	3×10^{7}	0.3	—

The experimental slope was reinforced by frame beams with anchor cables. To ensure a safety factor against slope instability exceeding 1.2 and following a rational calculation, an anchoring force of 600 kN was chosen. Appropriate spacing between anchor holes was determined to be 3 m horizontally and 4.25 m vertically. The prestressed anchor cables consisted of four high-strength, low-relaxation steel strands, each with a length of 25 m and a diameter of φ15.24.

2.2. Preparation and Assembly of the Frame Beams

Three types of frame beams were employed in the field test area to reinforce the slope: cast-in-situ frame beams, precast prestressed frame beams with connections, and precast prestressed frame beams. As depicted in Figure 1, each type of frame beam consisted of three columns of beams in the field test. Each frame beam was uniquely identified by its position, where FB-A-X represented the frame beams located in column A, row X, and FB is an abbreviation for the frame beam.

The cast-in-situ frame beams were integral structures comprising three vertical beams and two transverse beams, with specific dimensions as depicted in Figure 2, constructed using conventional building techniques. Conversely, precast prestressed frame beams were manufactured in the fabricated factory and applied prestress with each steel strand pre-tensioned to 15 t. After production completion, these precast prestressed frame beams were transported and hoisted into their respective positions, where prestressed anchor cables were applied. Precast prestressed frame beams and those with connections comprised three columns of beams, each consisting of two cross-shaped beams and one 1-shaped beam, with detailed dimensions illustrated in Figures 3–5. The connection method utilized for precast prestressed frame beams involved embedding connecting steel reinforcements at the ends of the frame beams. Once the precast prestressed frame beams were hoisted onto the slope and positioned, concrete was poured at the specified locations where the pre-embedded connecting steel reinforcements were located, effectively joining the three columns of the precast prestressed frame beams into a cohesive structure. This was followed by the application of prestressed anchor cables. The material parameters of frame beams are shown in Table 1.

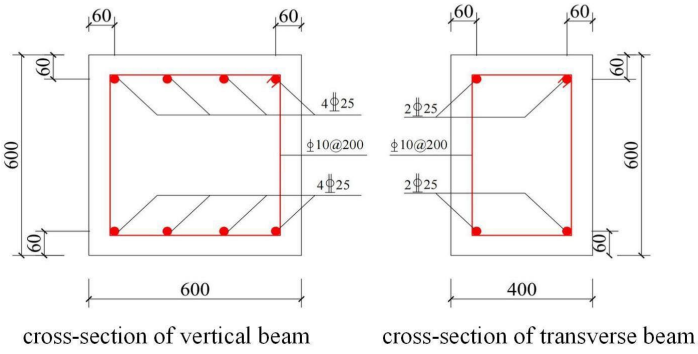


Figure 2. Reinforcements' layout of the cast-in-situ frame beam (unit: mm).

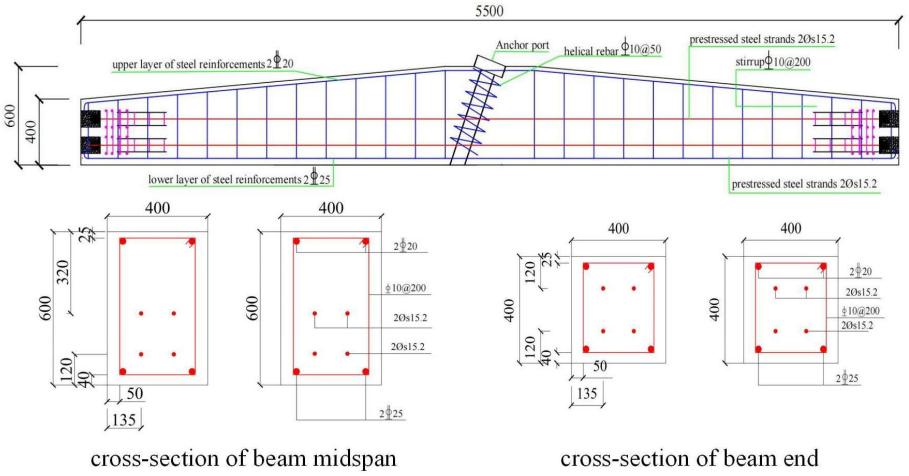


Figure 3. Reinforcements' layout of the longitudinal beam of the cross-shaped precast prestressed frame beams (unit: mm).

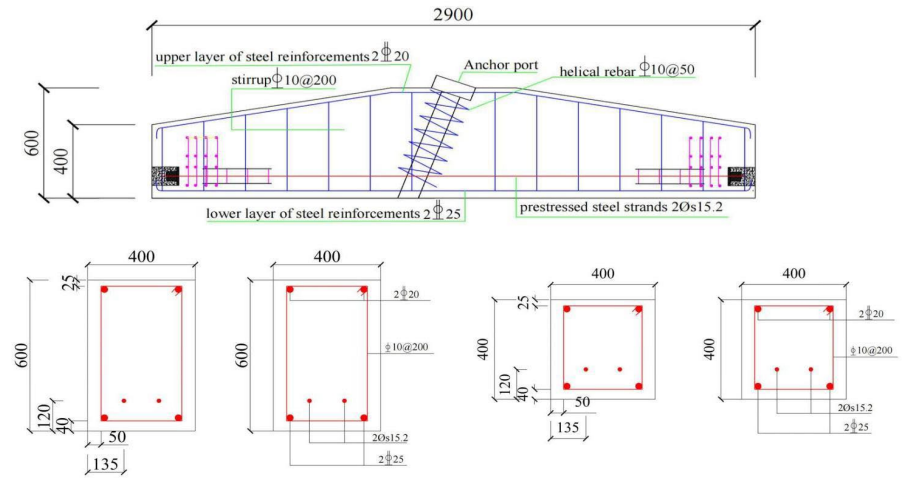


Figure 4. Reinforcements' layout of the transverse beam of the cross-shaped precast prestressed frame beams (unit: mm).

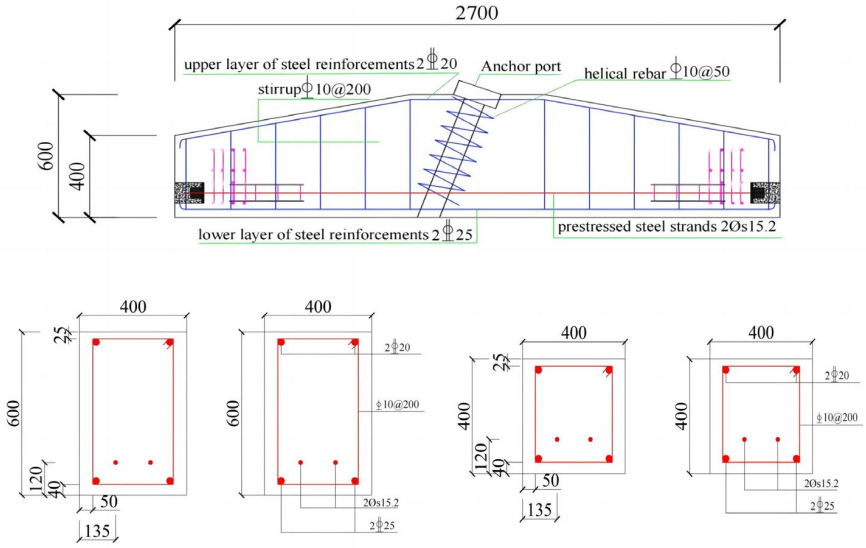


Figure 5. Reinforcements' layout of the 1-shaped precast prestressed beams (unit: mm).

2.3. Experiment Design

Each column of beams was equipped with three anchor ports, and the prestressed anchor cables consisted of four high-strength, low-relaxation steel strands, each with a length of 25 m and a diameter of φ15.24. The maximum anchoring force applied to frame beams was 600 kN, following a loading sequence: 160 kN–240 kN–320 kN–360 kN–400 kN–600 kN. Vibrating wire anchor load cells were positioned at each anchor port to measure the anchoring forces applied to the frame beams. Additionally, to monitor the forces in the longitudinal steel reinforcement within the frame beams, 180 vibrating wire strain gauges were utilized, with the locations of the measurement points illustrated in Figure 6, and stresses obtained through the sensors could be converted into steel reinforcement forces and section bending moments.

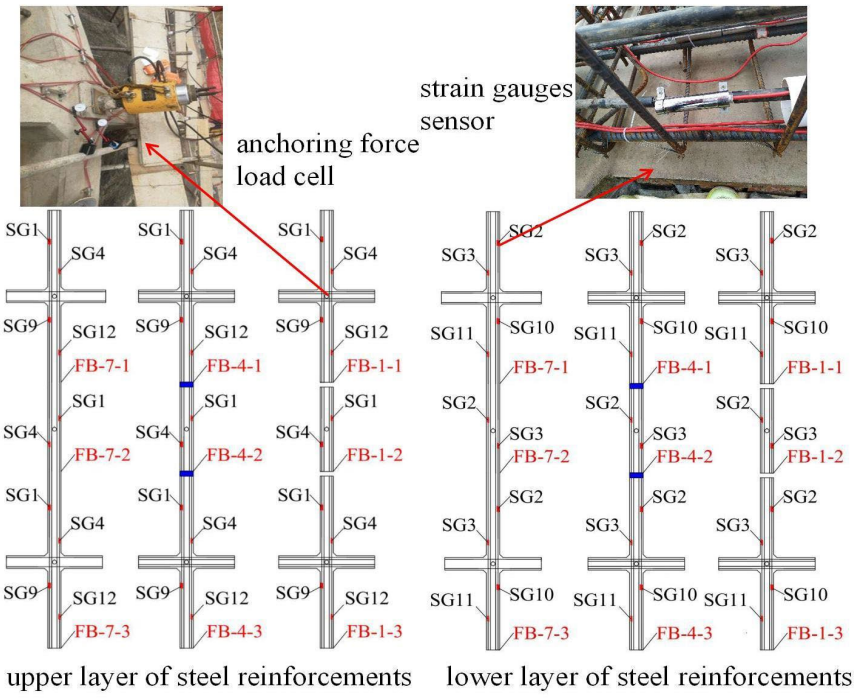
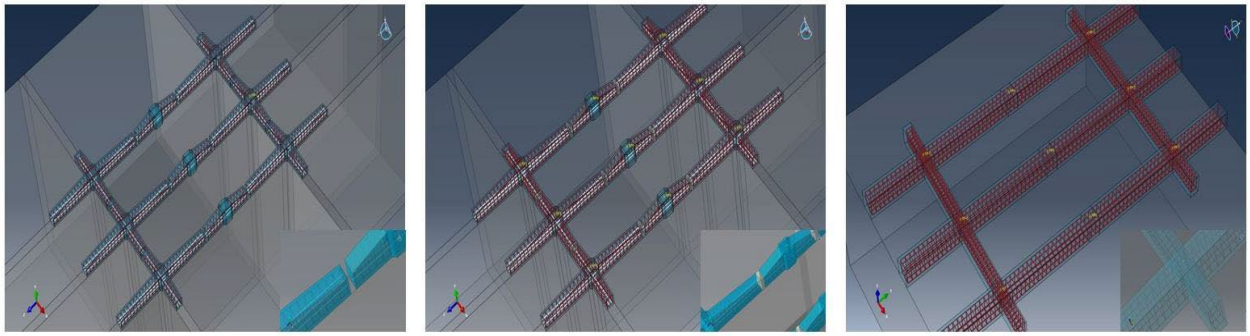


Figure 6. Schematic diagram of sensor positions.

3. Numerical Study

In this study, the performance of three types of frame beams under a 600 kN anchoring force was analyzed using the general finite element analysis software ABAQUS 2020. The frame beams and slope were three-dimensionally modeled at a 1:1 scale to simulate the behavior of longitudinal steel reinforcements within the frame beams during the loading process, and the distribution of section bending moments within the frame beams under a 600 kN anchoring force.

In the numerical simulations, a static general analysis step was employed for the slope. The concrete beams were modelled using eight-node linear hexahedral elements (C3D8R), while steel reinforcements, prestressed steel strands, and anchor cables were represented using two-node linear truss elements (T3D2). The soil used the Mohr–Coulomb model, while the contact method between the soil and the frame beams was set as surface-to-surface contact. Boundary conditions: the x, y, z of the lower surface of the soil were completely constrained. Prestresses were achieved through changes in temperature. The mechanical parameters for the four material types in the model are outlined in Table 1. Figure 7 illustrates the numerical models for the precast prestressed frame beams, precast prestressed frame beams with connections, and the cast-in-situ frame beams.



(a) Numerical Model of Precast Prestressed Frame Beams

(b) Numerical Model of Precast Prestressed Frame Beams with Connections

(c) Numerical Model of Cast-in-situ Frame Beams

Figure 7. Numerical models of frame beams: (**a**) precast prestressed frame beams; (**b**) precast prestressed frame beams with connections; (**c**) cast-in-situ frame beams.

4. Results and Discussions

4.1. The Analysis of Steel Reinforcement Forces

The study focuses on the experimental beams identified as FB-1-X, FB-4-X, and FB-9-X, representing the precast prestressed frame beams, the precast prestressed frame beams with connections, and the cast-in-situ frame beams, respectively. Figures 8 and 9 depict the force behavior of the longitudinal steel reinforcements in the three types of frame beams during the loading process of prestressed anchoring cables up to 600 kN. These results were obtained from both the field test and numerical simulations. It should be noted that the force was considered positive when it represented pressure and negative when it represented tension.

(1) As the anchoring force increased, the forces in the upper layer of the longitudinal steel reinforcements in all three types of frame beams increased linearly. Additionally, the forces in the lower layer of the longitudinal steel reinforcements decreased linearly. This observation implies that the three types of frame beams remained within the elastic deformation range under a 600 kN anchoring force, meeting the design load capacity requirements. It is worth noting that the volume of precast prestressed frame beams was only 57% of that of the cast-in-situ frame beams. Under the anchoring force, the upper layer steel reinforcements experienced pressure, while the lower layer steel reinforcements underwent tension.

(2) In the absence of an anchoring force, the longitudinal steel reinforcement in the precast frame beams experienced pressure due to the presence of prestresses. The forces in

the longitudinal steel reinforcements for the precast prestressed frame beams with connections were slightly lower than those of the precast prestressed frame beams. This phenomenon could be attributed to the precast prestressed frame beams with connections acting as a unified whole, which facilitated pressure transmission.

(3) The discrepancy between the measured steel reinforcement forces and the numerical simulation values could be attributed to the fact that the numerical simulation did not account for prestress loss in the anchor cables during the calculation. To improve the accuracy of the numerical simulation, it would be appropriate to apply a suitable reduction factor to the anchoring force when studying the steel reinforcement forces of the frame beams with an anchoring force.

(4) The steel reinforcement forces obtained from the field test and numerical simulations closely matched, mutually validating the accuracy of the data.

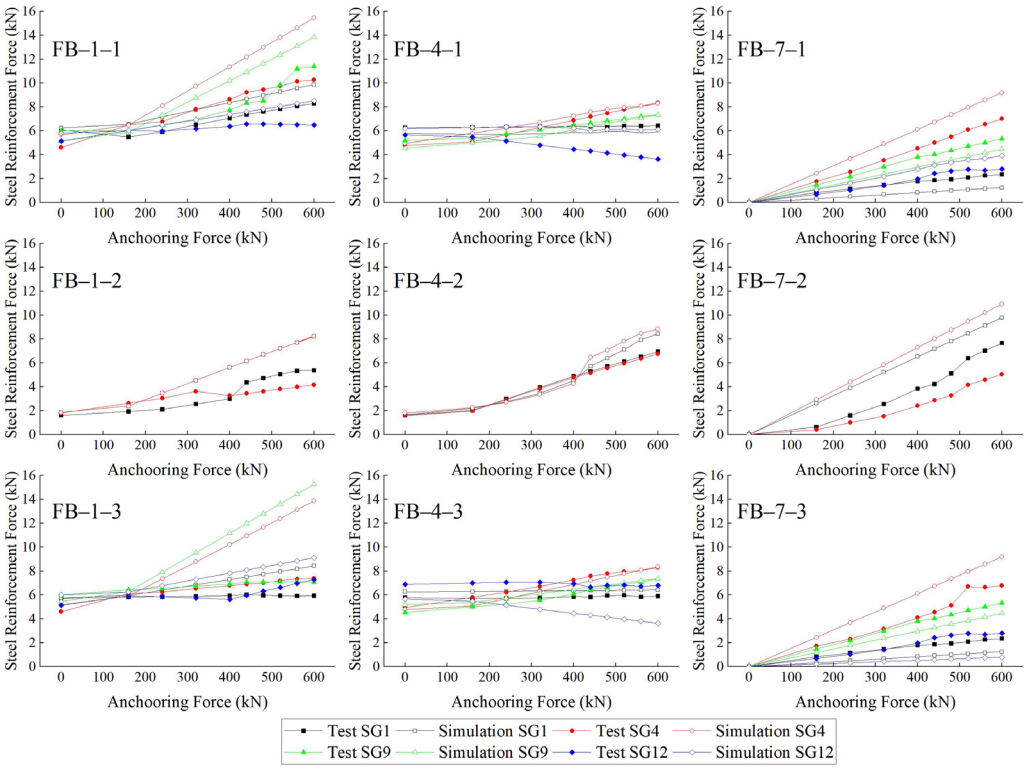


Figure 8. Upper layer of the steel reinforcement force.

4.2. The Analysis of Section Bending Moments

The study focuses on the experimental beams designated as FB-1-X, FB-4-X, and FB-9-X, representing the precast prestressed frame beams, the precast prestressed frame beams with connections, and the cast-in-situ frame beams, respectively. Regarding the time when the anchoring force was loaded up to 600 kN, Figure 10 presents a comparative chart of section bending moments for the three types of frame beams obtained from the field test and numerical simulations, and Figure 11 displays a comparative chart of section bending moments obtained from numerical simulations for three types of frame beams. In terms of bending moments, the upper portion of the beam experiencing tension and the lower portion experiencing pressure were considered positive bending moments, while the reverse was considered negative bending moments.

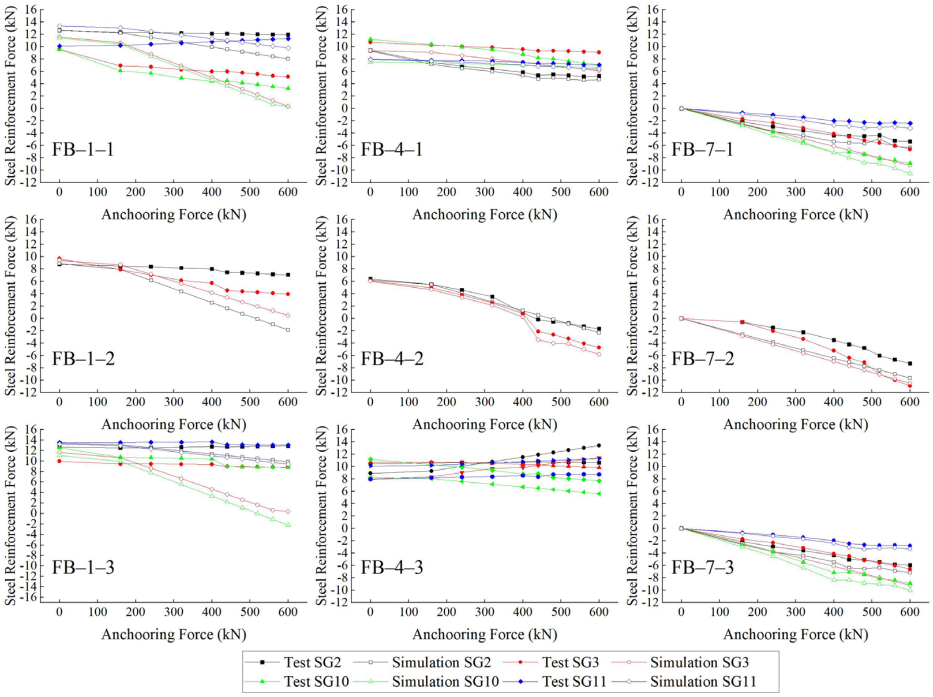


Figure 9. Lower layer of the steel reinforcement force.

(1) In Figure 10, the bending moments obtained from the field test and numerical simulations were in substantial agreement, validating the accuracy of the data. Notably, most measured section bending moments were generally higher than the numerical values. This discrepancy could be attributed to the numerical simulations not accounting for the loss of prestresses in the anchor cables and other unavoidable interfering factors in the field test, such as uneven soil distribution, frame beam disturbance, temperature, etc.

(2) Figure 10 indicates that the bending moment range for precast prestressed frame beams was −110 to −30 kN·m; for precast prestressed frame beams with connections, the range was from −70 to −20 kN·m; and for cast-in-situ frame beams, it fell within the range of −140 to −20 kN·m. This suggests that precast prestressed frame beams exhibited better load-bearing performance. This improvement could be attributed to the presence of prestresses in the precast frame beams, which could offset some bending moments generated by the anchoring force. Additionally, connecting all precast prestressed frames optimized their load-bearing performance.

(3) In Figure 11, it is evident that the maximum bending moment for all three types of frame beams occurred at the anchor point. Notably, the maximum bending moment for precast prestressed frame beams with connections was 60 kN·m smaller than that for cast-in-situ frame beams. This reduction was attributed to the bending moment generated by prestresses in the precast prestressed frame beams, countering a portion of the bending moment caused by the anchoring force.

(4) The maximum bending moment in the precast prestressed frame beams with connections was significantly lower than that in the precast prestressed frame beams. This phenomenon could be attributed to the precast prestressed frame beams with connections functioning as an integrated entity, facilitating the distribution and sharing of bending moments among the components. Consequently, the bending moment distribution in the precast prestressed frame beams with connections was more uniform.

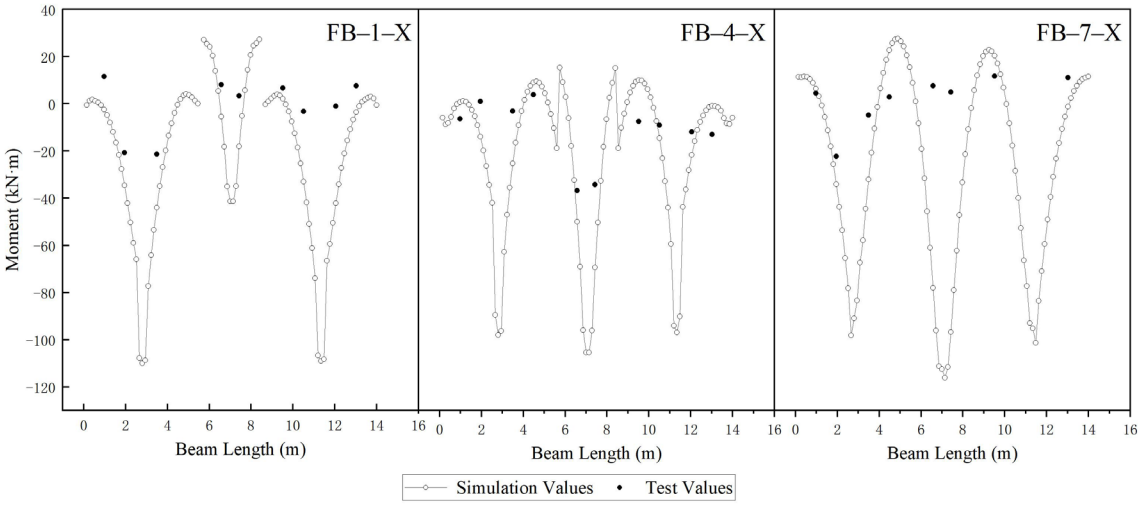


Figure 10. Comparison chart of measured bending moments and numerical bending moments.

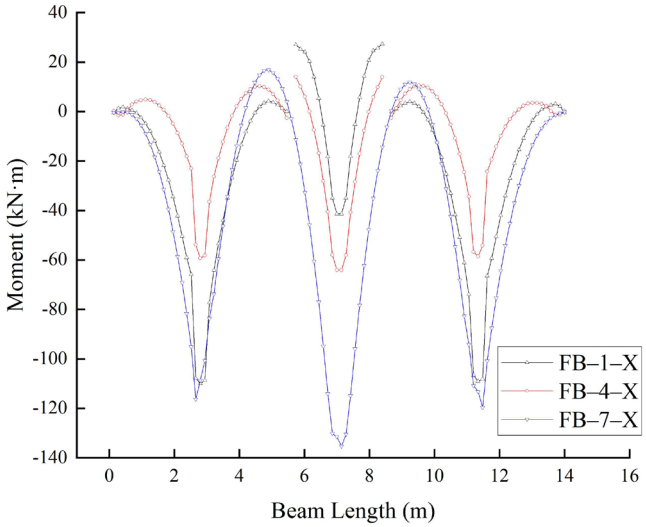


Figure 11. Comparative chart of numerical bending moments for the three types of frame beams.

5. Conclusions

This study, conducted through a field test in Yunnan, China and numerical simulations, investigated the load-bearing performance of three types of frame beams subjected to a 600 kN anchoring force during both loading and the normal service period. These frame beams included cast-in-situ frame beams, precast prestressed frame beams with connections, and precast prestressed frame beams. The following conclusions were drawn:

(1) The field test results closely aligned with the numerical values, affirming the reliability of the simulation approach employed in this study. This method can be extended to exploring diverse properties and characteristics of frame beams with anchor cables, thereby paving the way for further research in this field.

(2) Throughout the anchoring force loading process, all three types of frame beams remained within the elastic range; it was shown that three types of frame beams met the design requirements. However, it is crucial to emphasize that the volume of the precast frame beams was merely 57% of that of the cast-in-situ frame beams. Furthermore, the precast prestressed frame beams exhibited superior load-bearing performance. This improvement was primarily attributed to prestresses in the precast prestressed frame beams.

(3) When the anchoring force reached 600 kN, the maximum bending moment in the precast prestressed frame beams with connections was 60 kN·m less than that in the cast-in-situ frame beams. The reduction could be attributed to the bending moment generated by the prestresses in the precast prestressed frame beams, which counteracted a portion of the bending moment caused by the anchoring force.
(4) The precast prestressed frame beams with connections outperformed precast frame beams in terms of steel reinforcement forces and section bending moments. This improvement could be attributed to the precast prestressed frame beams with connections functioning as an integrated entity, allowing for the transfer of forces and bending moments at the connection points, resulting in a more even distribution of forces and moments.
(5) The numerical results of section bending moments were generally lower than the field test values. When using numerical simulation methods to study the bending moments of anchor frame beams, applying a suitable amplification factor to the numerical values may be appropriate.

Author Contributions: M.Q. and G.D. contributed equally to this paper and share first authorship. Conceptualization, M.Q. and G.D.; validation, M.Q., G.D, and S.W.; data curation, M.Q. and G.D.; writing—original draft preparation, M.Q. and J.Y.; writing—review and editing, J.Y. and S.W.; project administration, S.W.; funding acquisition, J.Y. All authors have read and agreed to the published version of the manuscript.

Funding: This research was funded by Science and Technology Project of Yunnan Provincial Department of Transportation, China, [2020]: No. 116.

Data Availability Statement: The data presented in this study are available on request from the corresponding author.

Conflicts of Interest: Author Shaowei Wei was employed by China Academy of Railway Sciences Corporation Limited and Beijing Tieke Special Engineering Technological Development Corporation Limited. The remaining authors declare that the research was conducted in the absence of any commercial or financial relationships that could be construed as a potential conflict of interest.

References

1. Choi, K.Y.; Cheung, R.W.M. Landslide disaster prevention and mitigation through works in Hong Kong. *J. Rock Mech. Geotech. Eng.* **2013**, *5*, 354–365. [CrossRef]
2. Yang, G.; Zhong, Z.; Zhang, Y.; Fu, X. Optimal design of anchor cables for slope reinforcement based on stress and displacement fields. *J. Rock Mech. Geotech. Eng.* **2015**, *7*, 411–420. [CrossRef]
3. Lin, Y.Y.; Li, Y.; Guolin, Y.; Li, Y. Experimental and numerical study on the seismic behavior of anchoring frame beam supporting soil slope on rock mass. *Soil Dyn. Earthq. Eng.* **2017**, *98*, 12–23. [CrossRef]
4. Ge, Y.; Tang, H.; Ez Eldin, M.A.M.; Chen, H.; Zhong, P.; Zhang, L.; Fang, K. Deposit characteristics of the Jiweishan rapid long-runout landslide based on field investigation and numerical modeling. *Bull. Eng. Geol. Environ.* **2018**, *78*, 4383–4396. [CrossRef]
5. Deng, D.; Zhao, L.; Li, L. Limit-Equilibrium Analysis on Stability of a Reinforced Slope with a Grid Beam Anchored by Cables. *Int. J. Geomech.* **2017**, *17*, 06017013. [CrossRef]
6. Yan, M.; Xia, Y.; Liu, T.; Bowa, V.M. Limit analysis under seismic conditions of a slope reinforced with prestressed anchor cables. *Comput. Geotech.* **2019**, *108*, 226–233. [CrossRef]
7. Zhou, C.; Hu, Y.; Xiao, T.; Ou, Q.; Wang, L. Analytical model for reinforcement effect and load transfer of pre-stressed anchor cable with bore deviation. *Constr. Build. Mater.* **2023**, *379*, 131219. [CrossRef]
8. Ye, S.; Fang, G.; Ma, X. Reliability Analysis of Grillage Flexible Slope Supporting Structure with Anchors Considering Fuzzy Transitional Interval and Fuzzy Randomness of Soil Parameters. *Arab. J. Sci. Eng.* **2019**, *44*, 8849–8857. [CrossRef]
9. Li, C.; Wu, J.; Wang, J.; Li, X. Layout and length optimization of anchor cables for reinforcing rock wedges. *Bull. Eng. Geol. Environ.* **2015**, *75*, 1399–1412. [CrossRef]
10. Zhang, T.; Zheng, H.; Sun, C. Global method for stability analysis of anchored slopes. *Int. J. Numer. Anal. Methods Geomech.* **2018**, *43*, 124–137. [CrossRef]
11. Shi, K.; Wu, X.; Liu, Z.; Dai, S. Coupled calculation model for anchoring force loss in a slope reinforced by a frame beam and anchor cables. *Eng. Geol.* **2019**, *260*, 105245. [CrossRef]
12. Wu, L.; Huang, R. Numerical simulation and optimum design of anchor frame beam strengthening expansive soil roadcut slope. *Rock Soil Mech.* **2006**, *27*, 605–614. [CrossRef]

13. Lin, Y.; Cheng, X.; Yang, G.; Li, Y. Seismic response of a sheet-pile wall with anchoring frame beam by numerical simulation and shaking table test. *Soil Dyn. Earthq. Eng.* **2018**, *115*, 352–364. [CrossRef]
14. Ye, W.; Zhou, Y.; Ye, S. Analysis of Deformation and Stress Characteristics of Anchored-Frame Structures for Slope Stabilization. *Adv. Civ. Eng.* **2020**, *2020*, e8870802. [CrossRef]
15. Li, J.; Zhu, Y.; Ye, S.; Ma, X. Internal Force Analysis and Field Test of Lattice Beam Based on Winkler Theory for Elastic Foundation Beam. *Math. Probl. Eng.* **2019**, *2019*, 5130654. [CrossRef]
16. Yuan, P.; Liu, Y. Analysis on Slope Frame Ground Beam under Dynamic Action. *IERI Procedia* **2012**, *1*, 94–100. [CrossRef]
17. Fan, J.; Shi-jiao, Y.; Deng, B.; Sun, B.; Liu, T. A Comparison of Load Distribution Methods at the Node and Internal Force Analysis of the Lattice Beam Based on the Winkler Foundation Model. *Buildings* **2023**, *13*, 1731. [CrossRef]
18. Lian, J.; Wu, J.; Luo, Q. Theoretical analysis and optimization of frame protection to control shallow slope stability and soil erosion. *Transp. Geotech.* **2022**, *33*, 100724. [CrossRef]
19. Cai, F.; Ugai, K. Reinforcing mechanism of anchors in slopes: A numerical comparison of results of LEM and FEM. *Int. J. Numer. Anal. Methods Geomech.* **2003**, *27*, 549–564. [CrossRef]
20. Zheng, H.; Liu, D.F.; Li, C.G. Slope stability analysis based on elasto-plastic finite element method. *Int. J. Numer. Methods Eng.* **2005**, *64*, 1871–1888. [CrossRef]
21. Zhu, C.; He, M.; Karakus, M.; Zhang, X.; Tao, Z. Numerical simulations of the failure process of anaclinal slope physical model and control mechanism of negative Poisson's ratio cable. *Bull. Eng. Geol. Environ.* **2021**, *80*, 3365–3380. [CrossRef]
22. Zhu, H.; Xiang, Q.; Luo, B.; Du, Y.; Li, M. Evaluation of failure risk for prestressed anchor cables based on the AHP-ideal point method: An engineering application. *Eng. Fail. Anal.* **2022**, *138*, 106293. [CrossRef]
23. Steinle, A.; Bachmann, H.; Tillmann, M. *Precast Concrete Structures*; Wiley: Hoboken, NJ, USA, 2019.
24. Japan Precast Concrete Frame Association. *PC Frame Construction Design and Construction Guide*; PC Frame Association: Tokyo, Japan, 2012. (In Japanese)
25. Japan Precast Concrete Frame Association. *PC Frame Construction Standard Calculation Data*; PC Frame Association: Tokyo, Japan, 2012. (In Japanese)
26. Čajka, R.; Navrátil, J. Numerical Solution of Prestressed Foundation—Subsoil Interaction Using FEM. *Key Eng. Mater* **2020**, *832*, 81–88. [CrossRef]
27. Ye, Y.; Wei, S.; Cai, D.; Yang, J.; Wei, P.; Yue, C.; Wu, S. Calculation method for internal force and deformation of the prestressed I-beam on the elastic foundation. *Front. Earth Sci.* **2023**, *10*, 996876. [CrossRef]

Disclaimer/Publisher's Note: The statements, opinions and data contained in all publications are solely those of the individual author(s) and contributor(s) and not of MDPI and/or the editor(s). MDPI and/or the editor(s) disclaim responsibility for any injury to people or property resulting from any ideas, methods, instructions or products referred to in the content.